AMERICAN SOCIETY FOR MICROBIOLOGY | Journal of Virology®

PATHOGENESIS AND IMMUNITY

Clearance of Chikungunya Virus Infection in Lymphoid Tissues Is Promoted by Treatment with an Agonistic Anti-CD137 Antibody

Jun P. Hong,[a] Mary K. McCarthy,[e] Bennett J. Davenport,[e] Thomas E. Morrison,[e] Michael S. Diamond[a,b,c,d]

[a]Department of Medicine, Washington University School of Medicine, St. Louis, Missouri, USA
[b]Department of Pathology and Immunology, Washington University School of Medicine, St. Louis, Missouri, USA
[c]Department of Molecular Microbiology, Washington University School of Medicine, St. Louis, Missouri, USA
[d]Center for Human Immunology and Immunotherapy Programs, Washington University School of Medicine, St. Louis, Missouri, USA
[e]Department of Immunology and Microbiology, University of Colorado School of Medicine, Aurora, Colorado, USA

ABSTRACT CD137, a member of the tumor necrosis factor receptor superfamily of cell surface proteins, acts as a costimulatory receptor on T cells, natural killer cells, B cell subsets, and some dendritic cells. Agonistic anti-CD137 monoclonal antibody (MAb) therapy has been combined with other chemotherapeutic agents in human cancer trials. Based on its ability to promote tumor clearance, we hypothesized that anti-CD137 MAb might activate immune responses and resolve chronic viral infections. We evaluated anti-CD137 MAb therapy in a mouse infection model of chikungunya virus (CHIKV), an alphavirus that causes chronic polyarthritis in humans and is associated with reservoirs of CHIKV RNA that are not cleared efficiently by adaptive immune responses. Analysis of viral tropism revealed that CHIKV RNA was present preferentially in splenic B cells and follicular dendritic cells during the persistent phase of infection, and animals lacking B cells did not develop persistent CHIKV infection in lymphoid tissue. Anti-CD137 MAb treatment resulted in T cell-dependent clearance of CHIKV RNA in lymphoid tissue, although this effect was not observed in musculoskeletal tissue. The clearance of CHIKV RNA from lymphoid tissue by anti-CD137 MAb was associated with reductions in the numbers of germinal center B cells and follicular dendritic cells. Similar results were observed with anti-CD137 MAb treatment of mice infected with Mayaro virus, a related arthritogenic alphavirus. Thus, anti-CD137 MAb treatment promotes resolution of chronic alphavirus infection in lymphoid tissues by reducing the numbers of target cells for infection and persistence.

IMPORTANCE Although CHIKV causes persistent infection in lymphoid and musculoskeletal tissues in multiple animals, the basis for this is poorly understood, which has hampered pharmacological efforts to promote viral clearance. Here, we evaluated the therapeutic effects on persistent CHIKV infection of an agonistic anti-CD137 MAb that can activate T cell and natural killer cell responses to clear tumors. We show that treatment with anti-CD137 MAb promotes the clearance of persistent alphavirus RNA from lymphoid but not musculoskeletal tissues. This occurs because anti-CD137 MAb-triggered T cells reduce the numbers of target germinal center B cells and follicular dendritic cells, which are the primary reservoirs for CHIKV in the spleen and lymph nodes. Our studies help to elucidate the basis for CHIKV persistence and begin to provide strategies that can clear long-term cellular reservoirs of infection.

KEYWORDS adaptive immunity, alphavirus, pathogenesis, viral immunity

Citation Hong JP, McCarthy MK, Davenport BJ, Morrison TE, Diamond MS. 2019. Clearance of chikungunya virus infection in lymphoid tissues is promoted by treatment with an agonistic anti-CD137 antibody. J Virol 93:e01231-19. https://doi.org/10.1128/JVI.01231-19.

Editor Julie K. Pfeiffer, University of Texas Southwestern Medical Center

Address correspondence to Michael S. Diamond, diamond@wusm.wustl.edu.

Received 26 July 2019
Accepted 19 September 2019
Accepted manuscript posted online 2 October 2019
Published 26 November 2019

Targeting of CD137 with an agonistic monoclonal antibody (MAb) enhances the spontaneous and antibody (Ab)-dependent cell-mediated cytotoxicity of natural killer (NK) cells and the proliferation and survival of $CD8^+$ T cells. Anti-CD137 MAb also enhances antigen presentation by promoting costimulatory activity of dendritic cells (DCs) and by inhibiting the functions of regulatory T cells (1). Based on preclinical studies demonstrating anti-CD137 MAb as a promising cancer immunotherapy (2–6), human clinical trials that combine anti-CD137 MAb with conventional chemotherapies for the treatment of metastatic solid tumors, non-small-cell lung cancer, melanoma, non-Hodgkin's B cell lymphoma, colorectal cancer, and multiple myeloma have been initiated (1).

Chikungunya virus (CHIKV) is a reemerging alphavirus of the *Togaviridae* family that is transmitted by *Aedes* species mosquitoes. CHIKV was first isolated in Tanzania in 1952 and has historically caused infections in Africa and Asia (7). In 2013, CHIKV spread into South and Central America, and an epidemic caused over 1.8 million infections, including cases in the United States (8). Infected individuals present with fever, rash, malaise, myalgia, and polyarthritis (9). Although symptoms can resolve within a few weeks, 30% to 60% of individuals report persistent musculoskeletal pain months to years after initial diagnosis (10–12). Indeed, CHIKV RNA and protein have been detected in perivascular synovial macrophages 18 months after infection (13). Persistent viral RNA in cells may act as a pathogen-associated molecular pattern (PAMP) and contribute to CHIKV-induced inflammation and arthritis (14–16).

In murine models of CHIKV, infectious virus is cleared from the blood and most tissues by 7 days postinfection (dpi). However, CHIKV RNA can be detected in musculoskeletal tissues, the spleen, and lymph nodes of immunocompetent mice for months (17). Although combinations of anti-CHIKV MAb with CTLA4-Ig, an immunomodulatory drug, controlled CHIKV arthritis in mice (18), antiviral antibody, alone or in combination with CTLA4-Ig, did not clear CHIKV RNA from sites of persistence when administered after infection. Based on studies in cancer models, we hypothesized that an agonistic anti-CD137 MAb could activate immune responses to resolve chronic viral infections. Here, we evaluated the activity of anti-CD137 MAb in a model of CHIKV arthritis in immunocompetent C57BL/6 mice. Treatment with an agonistic anti-CD137 MAb promoted clearance of persistent CHIKV RNA in the spleen and the draining lymph node (DLN), and this effect required the presence of T cells. However, clearance was not observed in musculoskeletal tissues. Viral RNA tropism studies revealed that B cells and follicular dendritic cells (FDCs) harbored much of the CHIKV RNA in lymphoid tissues. Unexpectedly, anti-CD137 MAb treatment resulted in reduced numbers of germinal center B cells and FDCs, compared with isotype-control MAb-treated animals. Thus, anti-CD137 MAb treatment cleared viral RNA in the spleen through either direct killing or indirect effects by T cells. As similar results were seen in mice with a second emerging alphavirus, Mayaro virus (MAYV), anti-CD137 MAb treatment resolves chronic alphavirus infection in lymphoid tissues by reducing the numbers of germinal center B cells and FDCs, which are the primary viral reservoirs in these tissues.

RESULTS

Anti-CD137 MAb treatment reduces CHIKV RNA levels in lymphoid but not musculoskeletal tissues. We hypothesized that agonistic anti-CD137 MAb might stimulate the immune system to clear chronic viral infections, analogous to its ability to reduce tumor burdens (1). To test this idea, we used a murine model of CHIKV infection. Four-week-old wild-type (WT) C57BL/6 male mice inoculated subcutaneously with CHIKV in the foot develop a biphasic pattern of joint swelling, with persistent viral RNA present in the musculoskeletal tissues of the ipsilateral and contralateral feet, the spleen, and the DLN (Fig. 1) (17); this viral RNA is maintained although infectious virus cannot be recovered after 7 dpi in immunocompetent mice (19). CHIKV-infected mice treated therapeutically with agonistic anti-CD137 MAb at 2 dpi developed increased foot swelling from 7 to 10 dpi, compared with isotype-control MAb-treated animals (Fig. 1A). Associated with this, we observed increased num-

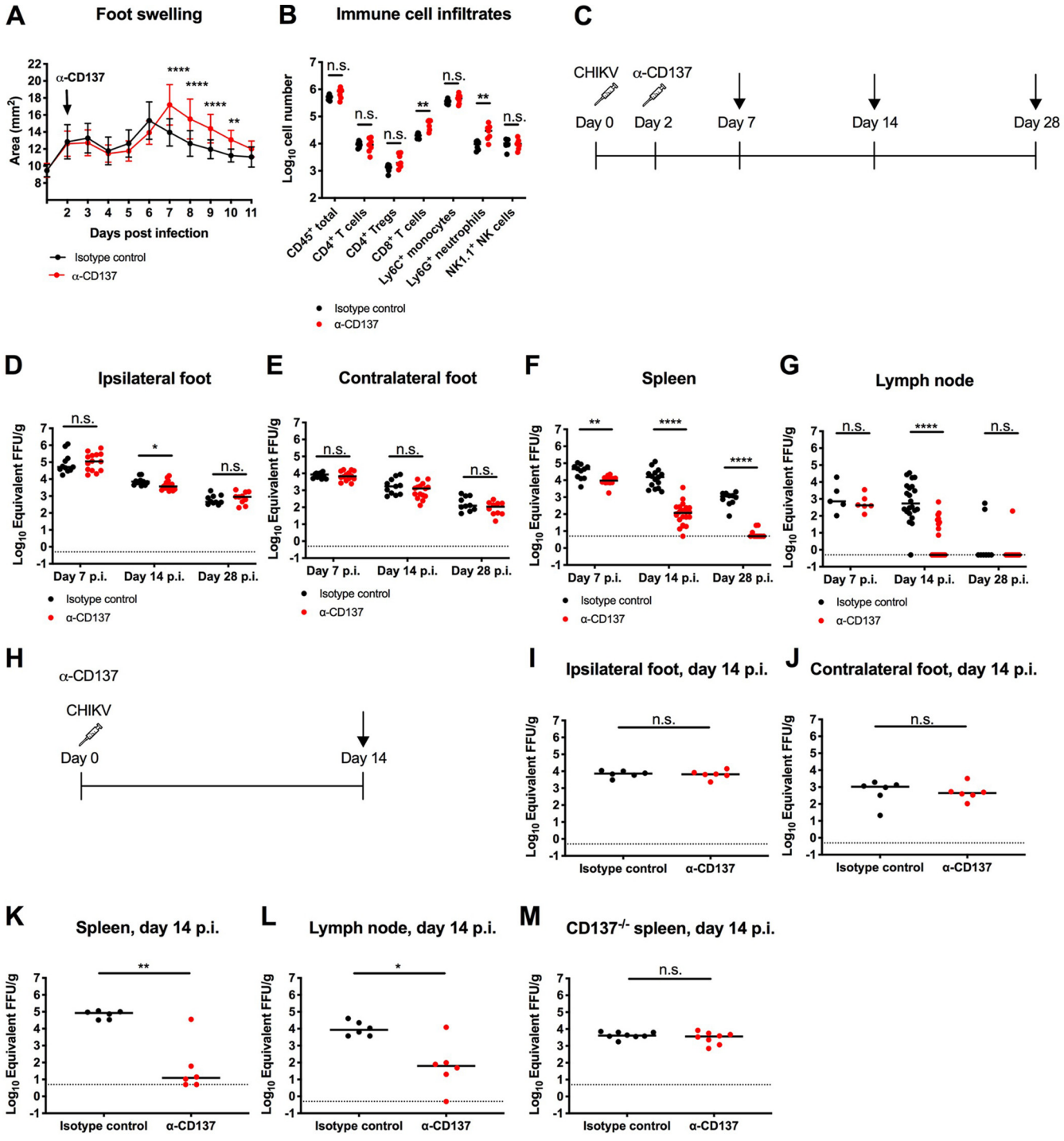

FIG 1 Anti-CD137 MAb treatment increases foot swelling but reduces viral RNA levels in the spleen and DLN. Four-week-old WT C57BL/6 male mice were inoculated with 10^3 FFU of CHIKV-LR at day 0. At 2 dpi, 400 μg of agonistic anti-CD137 MAb or isotype-control MAb was administered via the i.p. route. (A) Foot swelling was measured with digital calipers (15 to 18 mice per group). Each symbol represents the mean value for a group, and bars indicate standard deviations. **, $P < 0.01$; ****, $P < 0.0001$, two-way ANOVA with Šidák's posttest. (B) Ipsilateral feet were harvested at 7 dpi and processed for flow cytometry to quantify immune cell infiltrates. (C to G) The experimental scheme (C) shows that ipsilateral (D) and contralateral (E) feet, spleen (F), and DLN (G) were harvested at 7, 14, and 28 dpi. Viral RNA from tissue homogenates was measured by qRT-PCR. (H to L) The experimental scheme (H) shows that 400 μg of agonistic anti-CD137 MAb or isotype-control MAb was administered i.p. at the same time as virus inoculation, and ipsilateral (I) and contralateral (J) feet, spleen (K), and DLN (L) were harvested at 14 dpi. Viral RNA from tissue homogenates was measured by qRT-PCR. (M) Four-week-old CD137$^{-/-}$ C57BL/6 mice were inoculated with 10^3 FFU of CHIKV-LR at day 0. At 2 dpi, 400 μg of agonistic anti-CD137 MAb or isotype-control MAb was administered via the i.p. route. Spleens were harvested at 14 dpi, and viral RNA from tissue homogenates was measured by qRT-PCR. Each symbol represents an individual mouse, and bars indicate median values. Data in panels B, D to G, and I to M were pooled from two or three experiments. *, $P < 0.05$; **, $P < 0.01$; ****, $P < 0.0001$; n.s., not significant, Mann-Whitney test.

bers of $CD8^+$ T cells (3.3-fold; $P < 0.01$) and $Ly6G^+$ neutrophils (3.0-fold; $P < 0.01$) in the joints of anti-CD137 MAb-treated mice, compared with isotype-control MAb-treated animals, at 7 dpi (Fig. 1B).

Despite the changes in foot swelling induced by anti-CD137 MAb treatment, no differences in viral RNA levels were observed in the ipsilateral or contralateral foot at 7, 14, or 28 dpi (Fig. 1C to E). Similarly, the amount of CHIKV RNA in the ipsilateral or contralateral foot did not change, compared with isotype-control MAb-treated animals, at 14 dpi when mice were treated with anti-CD137 MAb at day 0, at the same time as virus inoculation (Fig. 1H to J).

Although anti-CD137 MAb treatment at 0 or 2 dpi failed to clear CHIKV RNA in musculoskeletal tissues, we observed reduced viral RNA levels in the spleen at 7 dpi, compared with isotype-control MAb treatment (Fig. 1F). At 14 and 28 dpi, anti-CD137 MAb-treated mice showed greater reductions in CHIKV RNA levels in the spleen (~130- to 220-fold; $P < 0.0001$) than isotype-control MAb-treated animals. In most animals (7 of 10 animals) treated with a single dose of anti-CD137 MAb at 2 dpi, viral RNA was not detected in the spleen at 28 dpi (Fig. 1F). Reduced levels of CHIKV RNA in the DLN (110-fold; $P < 0.0001$) also were observed at 14 dpi after anti-CD137 MAb treatment (Fig. 1G). At 28 dpi, however, CHIKV RNA in the DLN was absent in most anti-CD137 MAb-treated and isotype-control MAb-treated animals (Fig. 1G). When mice were treated with anti-CD137 MAb at 0 dpi, the amounts of CHIKV RNA in the spleen and the DLN at 14 dpi also were substantially reduced (140- to 7,000-fold; $P < 0.05$), compared with isotype-control MAb-treated animals (Fig. 1K and L). We confirmed the specificity of the effect; treatment of CHIKV-infected $CD137^{-/-}$ mice with agonistic anti-CD137 MAb at 2 dpi did not reduce viral RNA levels in the spleen (Fig. 1M).

Effect of anti-CD137 MAb on CHIKV tropism in the spleen. To begin to elucidate how anti-CD137 MAb treatment promoted clearance of CHIKV RNA in the spleen, we explored the cellular tropism of the virus in this tissue, which has remained undefined. Initially, we performed viral RNA *in situ* hybridization (ISH) with spleens from CHIKV-infected mice treated with anti-CD137 MAb or isotype-control MAb. At 7 dpi, much of the viral RNA was present in the center of lymphoid follicles of anti-CD137 MAb- or isotype-control MAb-treated animals (Fig. 2A and B). To define the cell types harboring CHIKV RNA, we sorted splenocyte subsets at 7 and 14 dpi by flow cytometry and performed quantitative reverse transcription-PCR (qRT-PCR); cells were fixed with paraformaldehyde (PFA) prior to sorting because of containment issues, as infectious CHIKV is a biosafety level 3 agent. At 7 and 14 dpi, FDCs and germinal center B cells contained the highest relative levels of CHIKV RNA, on a per-cell basis, in the spleens of isotype-control MAb-treated animals (Fig. 2C). When anti-CD137 MAb treatment was administered at 2 dpi, CHIKV RNA was preferentially cleared from FDCs at 7 dpi and was not appreciably detected in any splenocyte subsets at 14 dpi. During productive CHIKV infection, the subgenomic mRNA segment encoding the structural proteins (C-E3-E2-6K-E1) is preferentially transcribed, compared to the genomic RNA (20); this results in more copies of structural proteins, such as E1, than nonstructural proteins. As a surrogate assay for detection of infectious virus in the spleen, we measured the ratio of subgenomic RNA (E1 RNA) to genomic RNA (nsP2 RNA) by qRT-PCR. At least through 14 dpi, the ratio of E1 RNA to nsP2 RNA was greater than 1 (Fig. 2D to F), suggesting active infection.

In addition to altering CHIKV persistence in the spleen, we speculated that anti-CD137 MAb treatment might affect specific immune cell populations after infection. Anti-CD137 MAb treatment did not diminish the total number of leukocytes in the spleen (Fig. 3A), and we even observed a small increase (1.6-fold; $P < 0.01$) in the number of $CD3^+$ T cells at 14 dpi (Fig. 3B). However, we did observe a small decrease (1.4-fold; $P < 0.01$) in the number of $CD19^+$ B cells (Fig. 3C) and markedly reduced (up to ~40-fold; $P < 0.01$) numbers of peanut agglutinin-positive (PNA^+) $CD95^+$ or $GL7^+$ $CD95^+$ germinal center B cells and $CD45^-$ $CD54^+$ $CD21/CD35^+$ FDCs at 7 and 14 dpi (Fig. 3D to G). To test whether inhibition of germinal center development affected

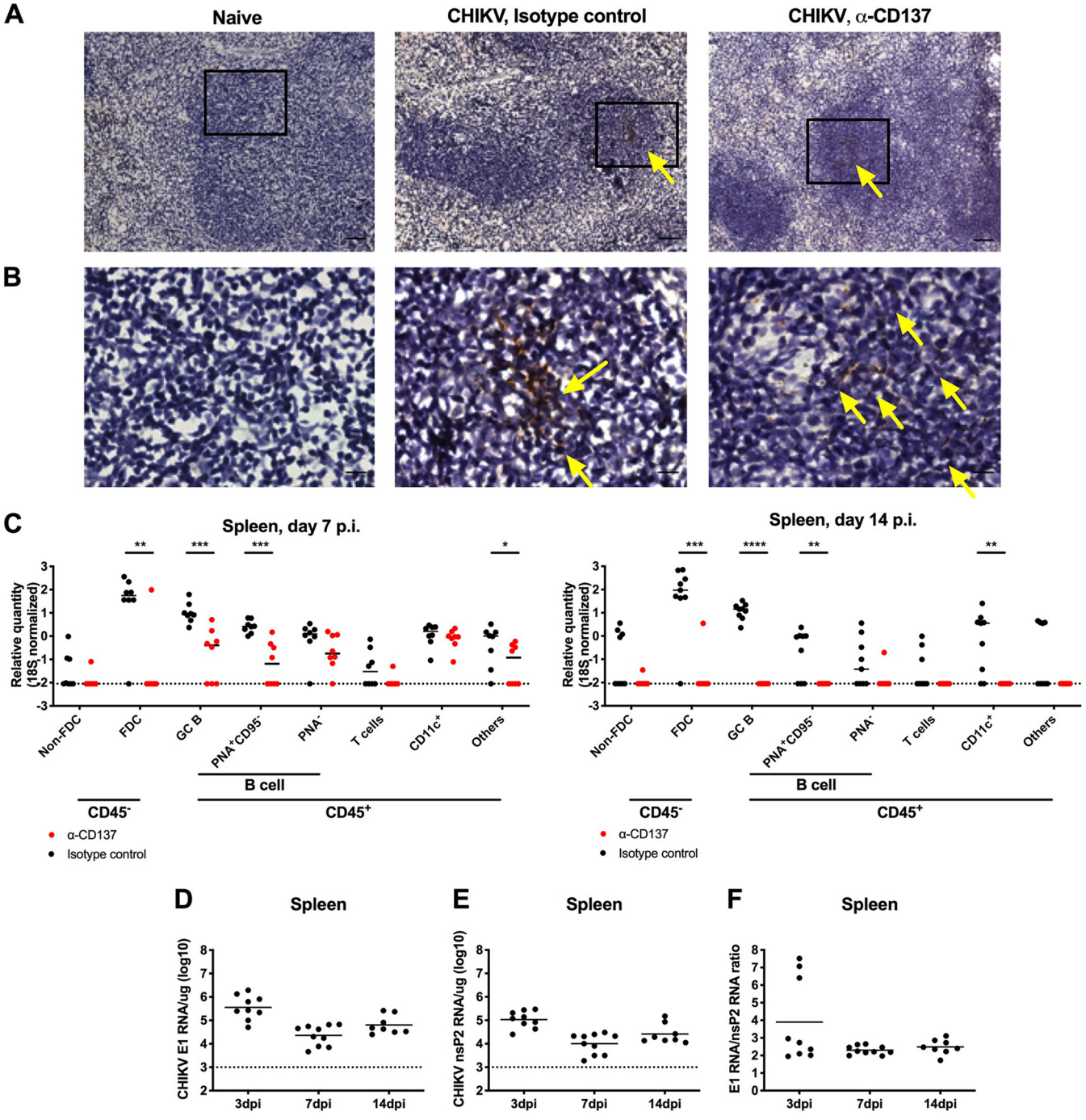

FIG 2 Germinal center (GC) B cells and FDCs harbor CHIKV viral RNA. Four-week-old WT C57BL/6 male mice were inoculated with 10^3 FFU of CHIKV-LR. At 2 dpi, 400 μg of agonistic anti-CD137 MAb or isotype-control MAb was administered via the i.p. route. (A) Spleens were harvested at 7 dpi, and viral RNA (brown) was visualized by ISH. Tissue sections were counterstained with Gill's hematoxylin. Scale bars, 50 μm. (B) Insets of panel A (black boxes) visualized at higher magnification. Scale bars, 10 μm. Yellow arrows indicate CHIKV RNA. (C) Spleens were harvested at 7 dpi (left) or 14 dpi (right), and bulk cells were fixed with PFA and sorted using flow cytometry. Viral RNA in each sorted cell subset was measured by qRT-PCR and normalized to 18S. (D to F) Four-week-old WT C57BL/6 male mice were inoculated with 10^3 PFU of CHIKV SL15649. Spleens were harvested at 3, 7, and 14 dpi, CHIKV E1 (D) and nsP2 (E) RNA from tissue homogenates was measured by qRT-PCR, and the ratio of E1 RNA to nsP2 RNA was calculated (F). Data were pooled from two experiments. Each symbol represents one mouse, and bars indicate median values. *, $P < 0.05$; **, $P < 0.01$; ***, $P < 0.001$; ****, $P < 0.0001$, Mann-Whitney test.

antiviral antibody responses, we measured anti-CHIKV IgG levels in the serum of infected mice at 30 dpi. Consistent with the reduced numbers of germinal center B cells, we observed lower (32-fold; $P < 0.001$) levels of anti-CHIKV IgG in anti-CD137 MAb-treated animals than in isotype-control MAb-treated animals (Fig. 3H).

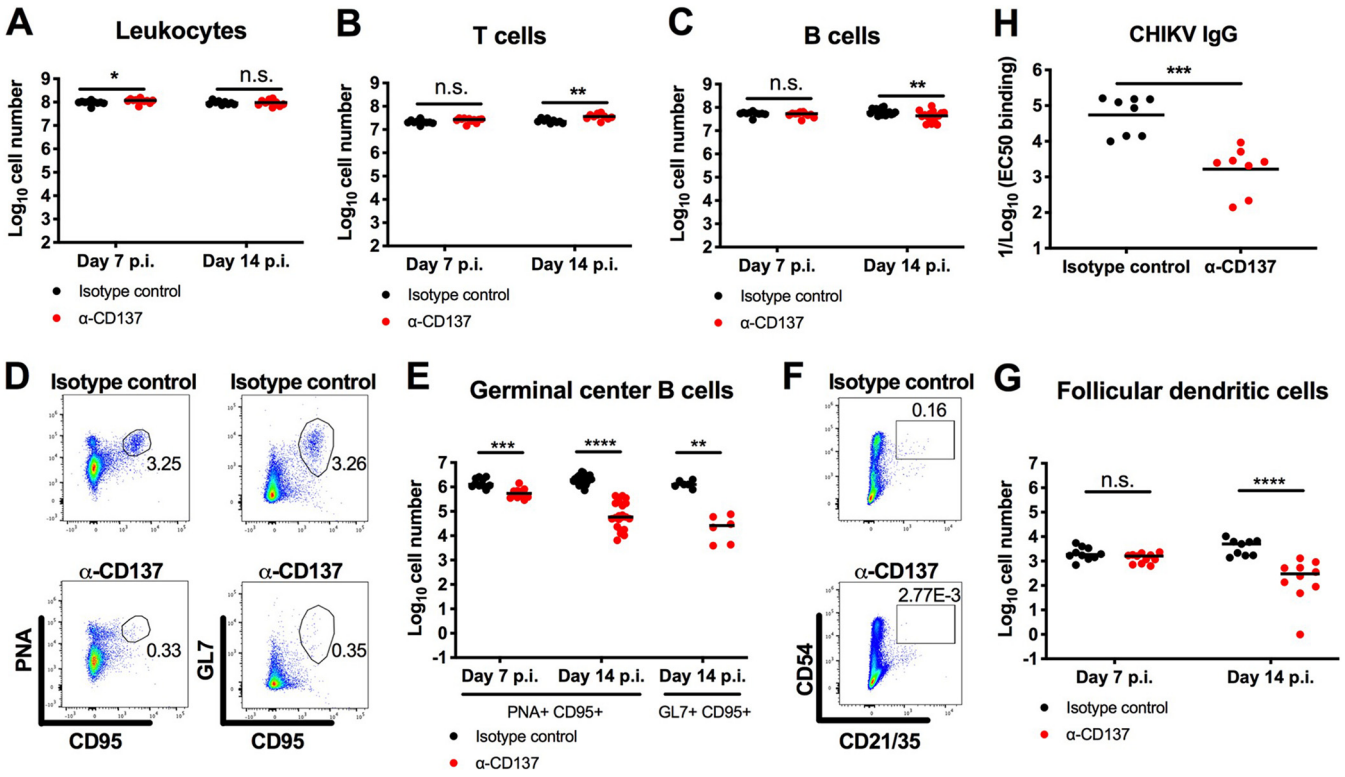

FIG 3 Anti-CD137 MAb treatment reduces the number of germinal center B cells and FDCs. Four-week-old WT C57BL/6 male mice were inoculated with 10^3 FFU of CHIKV-LR. At 2 dpi, 400 μg of agonistic anti-CD137 MAb or isotype-control MAb was administered via the i.p. route. (A to G) The numbers of total CD45$^+$ leukocytes (A), CD3$^+$ T cells (B), CD19$^+$ B cells (C), PNA$^+$ CD95$^+$ or GL7$^+$ CD95$^+$ germinal center B cells (D and E), and CD45$^-$ CD54$^+$ CD21/CD35$^+$ FDCs (F and G) in the spleen at 14 dpi were analyzed by flow cytometry. Representative flow cytometry dot plots of germinal center B cells (D) and FDCs (F) are shown. The numbers within the flow cytometry plots refer to the percentage of cells in the gated (boxed or circled) areas. (H) Serum was harvested at 30 dpi, and anti-CHIKV IgG titers were measured by ELISA. Each symbol represents an individual mouse, and bars indicate median values (with the exception of panel H, where mean values were used). Data were pooled from two or three experiments. *, $P < 0.05$; **, $P < 0.01$; ***, $P < 0.001$; ****, $P < 0.0001$; n.s., not significant, Mann-Whitney test.

B cells are required for persistence of CHIKV RNA in the spleen. Since splenic germinal center B cells and FDCs showed the greatest quantities of viral RNA, on a per-cell basis, after CHIKV infection, we further evaluated the contributions of these cells to the persistence of CHIKV RNA in the spleen. Initially, at 2 dpi we treated isotype-control MAb-treated mice with an anti-CD40L-blocking MAb, which inhibits the engagement of CD40L on B cells with its receptor CD40 on T helper cells and results in impaired germinal center formation (21). As expected, administration of CD40L-blocking MAb reduced the numbers of germinal center B cells and FDCs at 14 dpi, by 108- and 7-fold, respectively (Fig. 4A to D). This depletion was associated with an ~5-fold reduction in CHIKV RNA levels in the spleen, although the difference did not attain statistical significance (Fig. 4E, black circles). In comparison, treatment with anti-CD137 MAb in combination with CD40L-blocking MAb or the block-isotype-control MAb reduced viral RNA levels in the spleen, compared with treatment with isotype-control MAb in combination with CD40L-blocking MAb (123-fold; $P < 0.05$) or block-isotype-control MAb (660-fold; $P < 0.001$), respectively (Fig. 4E, black and red circles on the left or right, respectively). Collectively, these experiments show that, although germinal center B cells and FDCs in the spleens of isotype-control MAb-treated mice contain high levels of CHIKV RNA, other cell populations contribute to the persistence of CHIKV RNA.

Based on these data, we speculated that non-germinal center B cells also harbored CHIKV RNA in the spleen. Indeed, when we depleted all CD20$^+$ B cells using an anti-CD20 MAb at 2 dpi, we observed a 75-fold reduction ($P < 0.001$) in CHIKV RNA in the spleen at 14 dpi (Fig. 4F and G, black circles). To corroborate these data, B6.129S2-

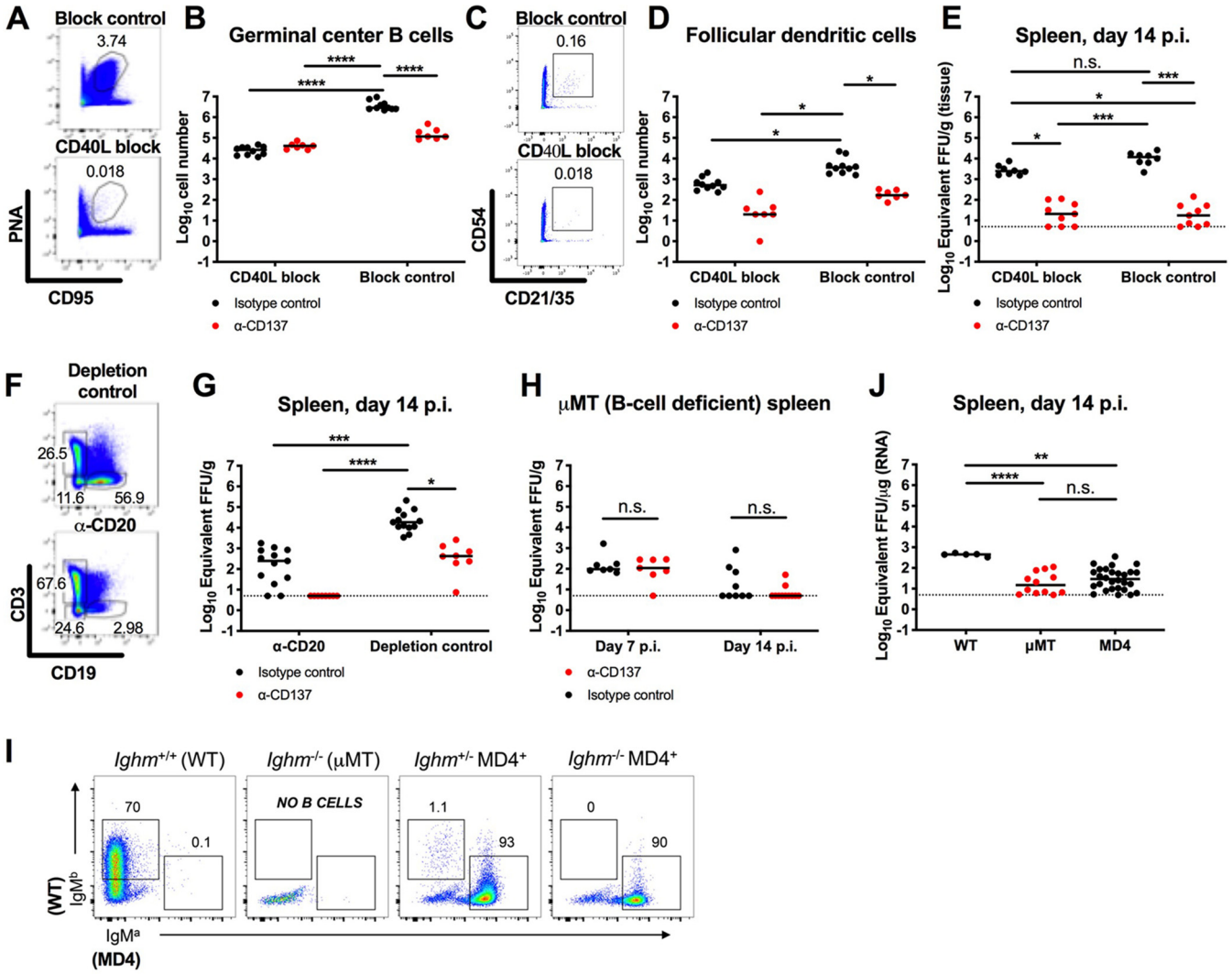

FIG 4 B cells are required for the persistence of CHIKV RNA in the spleen. (A to G) Four-week-old WT C57BL/6 male mice were inoculated with 10^3 FFU of CHIKV-LR. At 2 dpi, 400 μg of agonistic anti-CD137 MAb or isotype-control MAb in combination with CD40L-blocking MAb or block-isotype-control MAb (A to E) or anti-CD20 depleting MAb or depletion-isotype-control MAb (F and G) was administered via the i.p. route. Spleens were harvested at 14 dpi, and the numbers of PNA$^+$ CD95$^+$ germinal center B cells (A and B) and CD45$^-$ CD54$^+$ CD21/CD35$^+$ FDCs (C and D) were determined by flow cytometry. Representative flow cytometry dot plots of germinal center B cells (A), FDCs (C), and CD19$^+$ B cells (F) are shown. Viral RNA from tissue homogenates was measured by qRT-PCR (E and G). (H to J) Four-week-old μMT mice (H) or MD4 transgenic mice with a μMT background (I and J) were inoculated with 10^3 FFU of CHIKV-LR. For μMT mice (H), 400 μg of agonistic anti-CD137 MAb or isotype-control MAb was administered at 2 dpi. Spleens were harvested at 7 or 14 dpi, and viral RNA was measured. In panels H and J, each symbol represents an individual mouse, and bars indicate median values. *, $P < 0.05$; **, $P < 0.01$; ***, $P < 0.001$; ****, $P < 0.0001$; n.s., not significant, Kruskal-Wallis ANOVA with Dunn's posttest. At 14 dpi, the spleen was removed and processed for flow cytometry (I). Splenocytes were gated as B220$^+$ CD19$^+$ for B cells. Representative flow plots for each genotype are shown. WT B cells are IgM^{b+}, and HEL-specific (MD4) B cells are IgM^{a+}. MD4 B cells were also confirmed by staining with HEL (data not shown). Data were pooled from two to four experiments. In this figure, the numbers within the flow cytometry plots refer to the percentage of cells in the adjacent gated (boxed or circled) areas.

Ighm^{tm1Cgn}/J (μMT) (B cell-deficient) mice were inoculated with CHIKV and treated with anti-CD137 MAb at 2 dpi. Viral RNA levels at 7 dpi in the spleens of μMT mice were lower than those in WT mice with anti-CD137 MAb treatment (87-fold; $P < 0.001$) or without it (299-fold; $P < 0.001$) (Fig. 1F and Fig. 4H). However, the levels of viral RNA in the spleens of anti-CD137 MAb-treated and isotype-control MAb-treated μMT mice at 7 dpi were similar. At 14 dpi, almost no CHIKV RNA was detected in the spleens of these mice with or without anti-CD137 MAb treatment (Fig. 4H).

Antigen in the form of immune complexes can be captured by cells expressing Fcγ or complement receptors (CRs), or antigen can be directly captured by B cell receptors. We next tested whether CHIKV-specific antibody was required for the persistence of viral RNA in the spleen. To assess this, we used transgenic MD4 mice in a μMT

background; these mice have B cell receptors that are specific for only hen egg lysozyme (HEL) (Fig. 4I) (22). At 14 dpi, viral RNA was detected in the spleens of MD4 mice, albeit at substantially lower levels than in WT mice, whereas almost no viral RNA was measured in the spleens of μMT mice (Fig. 4J). Thus, the antigen specificity of B cells contributes to the persistence of CHIKV RNA in the mouse spleen.

T cells are required for anti-CD137-mediated clearance of CHIKV in the spleen. We hypothesized that the agonistic anti-CD137 MAb cleared CHIKV RNA in lymphoid tissues by activating CD137$^+$ immune cells with effector activity (1). By flow cytometry, we detected CD137 expression on splenic CD4$^+$ and CD8$^+$ T cells, NK cells, and natural killer T (NKT) cells in CHIKV-infected mice at 2 dpi (Fig. 5). To define the cells responsible for anti-CD137 MAb-mediated clearance of CHIKV RNA, we performed anti-CD137 MAb treatment experiments in mice depleted of NK cells, CD8$^+$ T cells, CD4$^+$ T cells, or neutrophils. Administration of anti-CD137 MAb in NK cell-, CD8$^+$ T cell-, or CD4$^+$ T cell-depleted mice resulted in diminished CHIKV RNA levels in the spleen at 14 dpi, although the reductions were only 2- to 5-fold lower than with control nondepleting MAbs (Fig. 6A to F). Ab-mediated depletion of both CD4$^+$ and CD8$^+$ T cells resulted in 9-fold less clearance effect of anti-CD137 MAb (Fig. 6G and H). Similarly, Ab-mediated triple depletion of CD4$^+$ and CD8$^+$ T cells and NK cells resulted in 21-fold less clearance by anti-CD137 MAb (Fig. 6I and J). In comparison, depletion of neutrophils did not affect anti-CD137 MAb-mediated clearance of CHIKV RNA in the spleen at 14 dpi (Fig. 6K and L). Consistent with a dominant role for CD3$^+$ cells in mediating clearance of CHIKV RNA in the spleen, the effect of anti-CD137 MAb was abolished completely in B6.129P2-Tcrb^{tm1Mom} Tcrd^{tm1Mom}/J (TCR$\beta\delta^{-/-}$) mice, which lack all T cell and NKT cell subsets (Fig. 6M).

Anti-CD137 MAb treatment reduces MAYV RNA levels. We assessed the effect of anti-CD137 MAb on a second alphavirus, MAYV, to determine whether the clearance phenotype was specific to CHIKV. In contrast to findings observed with CHIKV-infected mice, treatment with anti-CD137 MAb reduced (8-fold; $P < 0.0001$) viral RNA levels in the ipsilateral foot of MAYV-infected mice at 14 dpi (Fig. 7A), although viral RNA levels in the contralateral foot of anti-CD137 MAb-treated and isotype-control MAb-treated mice were similar (Fig. 7B). Similar to CHIKV-infected mice, anti-CD137 MAb treatment resulted in markedly reduced MAYV RNA levels in the spleen (241-fold; $P < 0.0001$) and DLN (5,962-fold; $P < 0.001$) at 14 dpi (Fig. 7C and D). Thus, anti-CD137 MAb-mediated clearance of viral RNA in lymphoid tissues occurred in the context of multiple alphavirus infections in mice, whereas reduction of viral RNA in musculoskeletal tissues was virus type specific.

DISCUSSION

In this study, we observed that agonistic anti-CD137 MAb administered at 2 dpi cleared CHIKV RNA in the spleen and DLN by 28 dpi, although viral RNA in musculoskeletal tissues of the foot persisted. In a parallel model of infection with MAYV, another arthritogenic alphavirus, anti-CD137 MAb treatment also reduced MAYV RNA levels in the spleen and DLN by 14 dpi. In the MAYV model, however, a partial clearance effect was observed in the ipsilateral foot but not the contralateral foot. Based on our cell-sorting and tropism data, germinal center B cells and FDCs were associated with the highest levels of viral RNA in the spleen, on a per-cell basis, at 7 and 14 dpi. Flow cytometric analysis revealed that anti-CD137 MAb treatment reduced the numbers of germinal center B cells and FDCs, and this was associated with diminished anti-CHIKV IgG responses. Inhibition of germinal center formation by anti-CD137 MAb also was observed in mice immunized with sheep red blood cells or keyhole limpet hemocyanin (23). When B cells were depleted using anti-CD20 MAb, CHIKV RNA levels in the spleen also were reduced at 14 dpi. Together, these data suggest a key role for B cells in maintaining persistent CHIKV RNA in the spleen. Consistent with these results, μMT mice lacking B cells had almost no detectable viral RNA in the spleen at 14 dpi, and MD4 transgenic mice, which have B cells specific for HEL, also had less CHIKV RNA in the spleen at 14 dpi. These data suggest that antigen-specific B cells are responsible for the

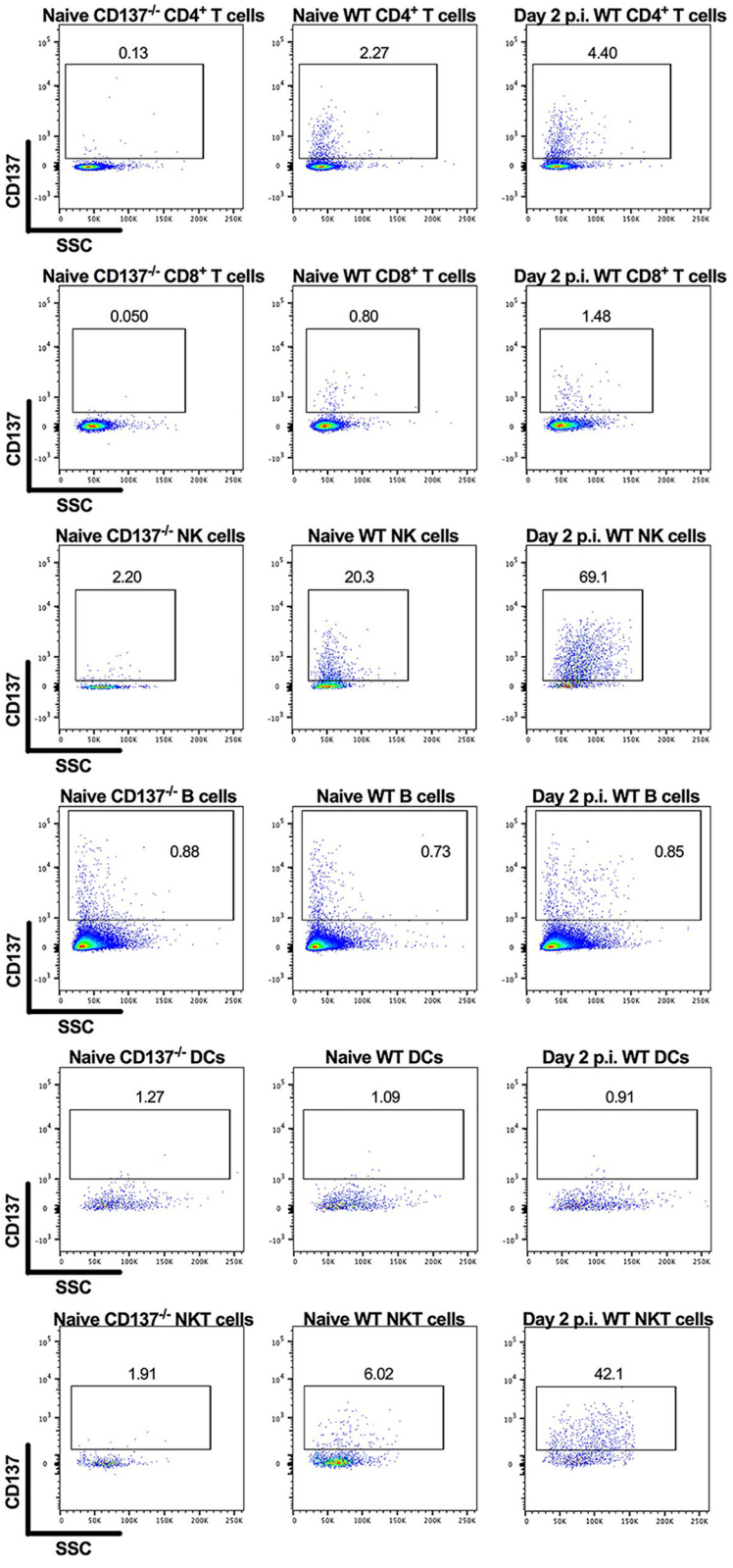

FIG 5 CD137 is expressed on splenic $CD4^+$ and $CD8^+$ T cells, NK cells, and NKT cells in CHIKV-infected mice at 2 dpi. Four-week-old WT C57BL/6 mice were inoculated with 10^3 FFU of CHIKV-LR at day 0. At 2 dpi, spleens were harvested and processed for flow cytometry. Flow cytometry dot plots show CD137 expression levels on $CD4^+$ and $CD8^+$ T cells, CD3-$NK1.1^+$ NK cells, $CD19^+$ B cells, MHC-II^+ $CD11c^+$ DCs, and $CD3^+$ $NK1.1^+$ NKT cells. Data are representative of two experiments. The numbers within the flow cytometry plots refer to the percentage of cells in the gated (boxed) areas.

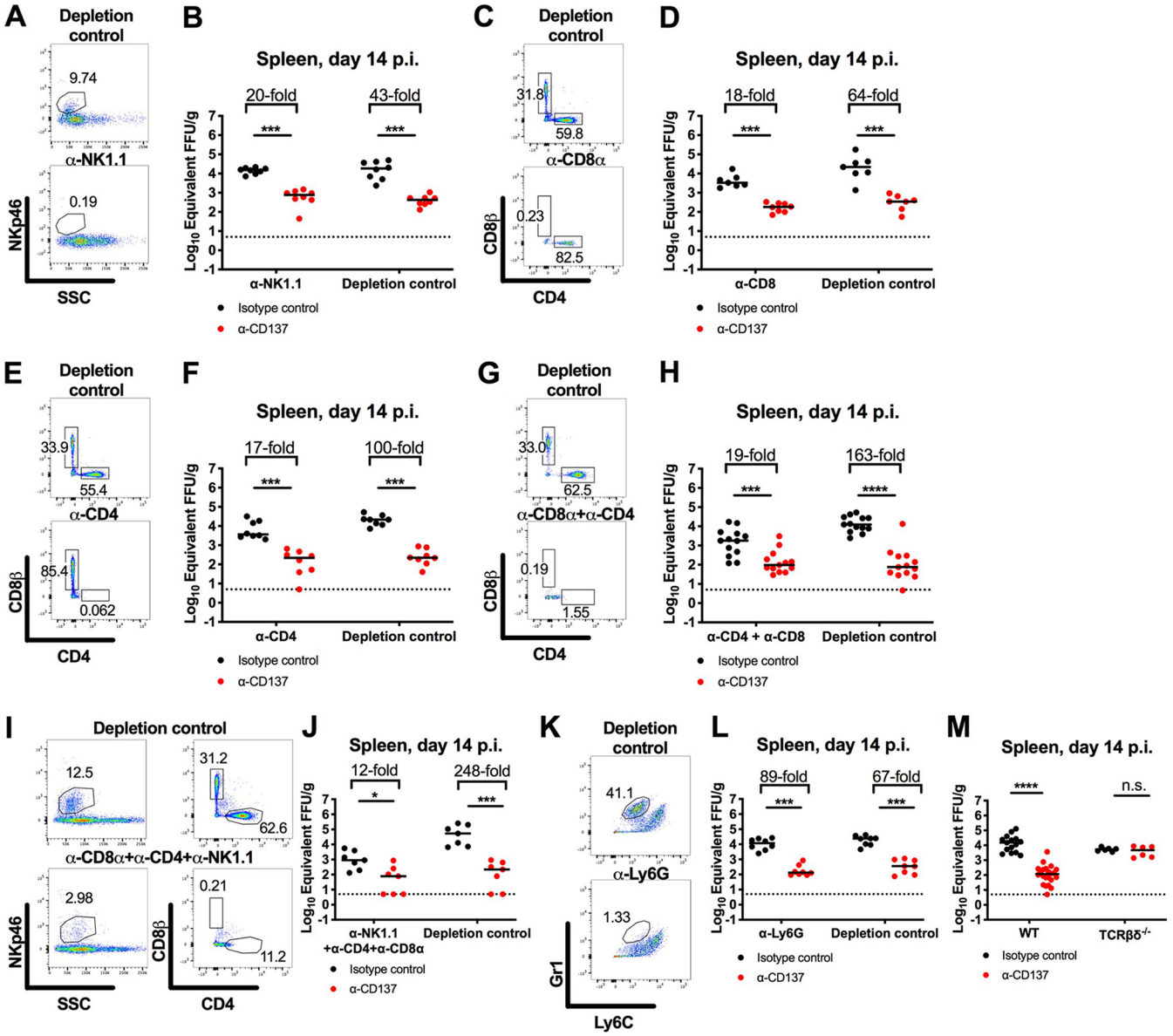

FIG 6 Anti-CD137 MAb-mediated clearance of CHIKV RNA in the spleen is abolished in mice lacking T cells. Four-week-old WT (A to L) or TCR$\beta\delta^{-/-}$ C57BL/6 (M) mice were inoculated with 10^3 FFU of CHIKV-LR. At 2 dpi, 400 μg of agonistic anti-CD137 MAb or isotype-control MAb in combination with anti-NK1.1 depleting MAb or depletion-isotype-control MAb (A and B), anti-CD8α depleting MAb or depletion-isotype-control MAb (C and D), anti-CD4 depleting MAb or depletion-isotype-control MAb (E and F), anti-CD8α and anti-CD4 depleting MAbs or depletion-isotype-control MAbs (G and H), anti-CD8α, anti-CD4, and anti-NK1.1 depleting MAbs or depletion-isotype-control MAbs (I and J), or anti-Ly6G depleting or depletion-isotype-control MAb (K and L) was administered via the i.p. route. All depleting and depletion-isotype-control MAbs were administered every 4 days, except for anti-Ly6G and isotype-control MAbs, which were administered every 2 days. Spleens were harvested at 14 dpi, and viral RNA from tissue homogenates was measured by qRT-PCR. Data were pooled from two or three experiments. Each symbol represents an individual mouse, and bars indicate median values. *, $P < 0.05$; ***, $P < 0.001$; ****, $P < 0.0001$; n.s., not significant, Mann-Whitney test. Representative flow cytometry dot plots confirming cell depletions are shown (A, C, E, G, I, and K). The numbers within the flow cytometry plots refer to the percentage of cells in the gated (boxed or circled) areas.

persistence of CHIKV RNA in mouse spleen. Anti-CD137 MAb-mediated clearance of CHIKV RNA in the spleen was diminished in anti-NK1.1-, anti-CD4-, and anti-CD8-treated mice and was abrogated in TCR$\beta\delta^{-/-}$ mice, which lack CD4$^+$ and CD8$^+$ T cells, NKT cells, and $\gamma\delta$ T cells in the spleen. Thus, anti-CD137 MAb-mediated clearance of CHIKV in lymphoid tissues is dependent primarily on T cells.

The basis of CHIKV RNA persistence in musculoskeletal tissues of infected animals remains a longstanding question in the field. Although anti-CD137 MAb treatment had marked effects in lymphoid tissues, it did not significantly alter CHIKV RNA levels in the

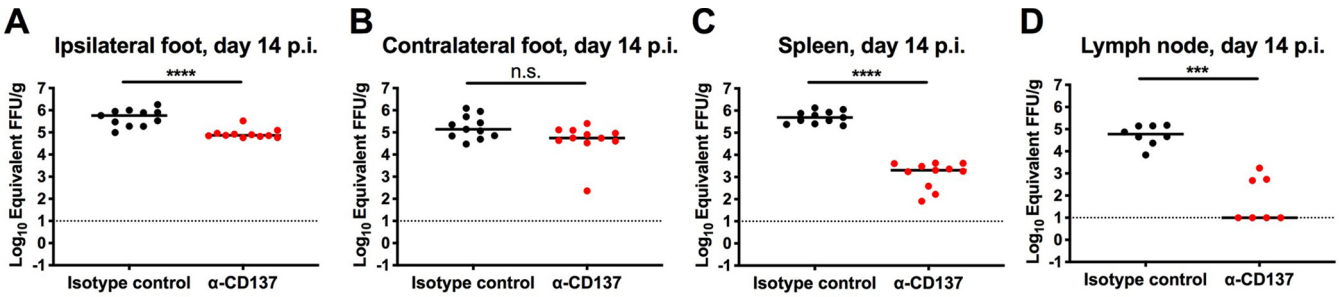

FIG 7 Anti-CD137 MAb treatment reduces levels of MAYV RNA in the spleen, DLN, and ipsilateral foot. Four-week-old WT C57BL/6 male mice were inoculated with 10^3 FFU of MAYV BeH407. At 2 dpi, 400 μg of agonistic anti-CD137 MAb or isotype-control MAb was administered via the i.p. route. Ipsilateral (A) and contralateral (B) feet, spleen (C), and DLN (D) were harvested at 14 dpi. Viral RNA from tissue homogenates was measured by qRT-PCR. Each symbol represents an individual mouse, and bars indicate median values. Data were pooled from three experiments. ***, $P < 0.001$; ****, $P < 0.0001$; n.s., not significant, Mann-Whitney test.

ipsilateral foot or the contralateral foot at 7, 14, or 28 dpi. The lack of CHIKV RNA clearance in the musculoskeletal tissues after anti-CD137 MAb treatment may be due to the distinct viral tropism in these tissues. During the acute phase of infection, CHIKV is readily detected in skeletal muscle cells, synovial fibroblasts, and other nonhematopoietic cells in mice (24, 25). During the chronic phase, the reservoir of CHIKV in muscle and joint tissues is less clear, although experiments with a Cre recombinase CHIKV strain and reporter mice showed that fibroblasts and skeletal muscle cells harbored persistent viral RNA (25). In contrast to our observations in the CHIKV model, agonistic anti-CD137 MAb treatment reduced viral RNA levels in the ipsilateral foot in the MAYV model. Although further study is warranted, the cellular tropism of MAYV may differ from that of CHIKV, as has been reported for other arthritogenic alphaviruses, such that additional infected cell types can be cleared by anti-CD137-activated T cells (26).

Our experiments showed that, in the spleen, germinal center B cells and FDCs were associated with high levels of CHIKV RNA at 7 and 14 dpi. Although viral RNA was readily detected, we did not recover infectious CHIKV from lymphoid tissues at those time points, as judged by plaque- or focus-forming assays. Notwithstanding these data, we observed higher E1/nsP2 RNA ratios, consistent with productive CHIKV infection. Additionally, B cells may capture CHIKV immune complexes via surface CRs and Fcγ receptors and transport it to FDCs in the B cell follicles (27, 28). Marginal zone B cells continuously shuttle between marginal zone and follicular areas, which can facilitate antigen transport (28). Alternatively, immune complexes taken up by subcapsular sinus or marginal zone macrophages can be transferred to CR2-expressing B cells, which then transport the immune complexes to CR2-expressing FDCs (29).

FDCs are thought to retain opsonized antigen for extended periods and present it to cognate B cells to form germinal centers (30). As an example, human FDCs isolated from patients retain HIV within nondegradative cycling compartments for long periods (31). Clearance of CHIKV RNA in the spleen after anti-CD137 MAb treatment correlated with reductions in the number of germinal center B cells and FDCs. Moreover, the levels of viral RNA in the spleen were reduced in μMT or MD4 transgenic mice lacking CHIKV-specific B cells and Abs. Based on our tropism analysis, blocking studies with anti-CD40L MAb, depletion studies with anti-CD20 MAb, and infection experiments in μMT B cell-deficient mice, it appears that multiple subtypes of B cells and FDCs retain much of the CHIKV RNA in lymphoid tissues during the subacute and chronic phases of infection.

Antitumor mechanisms of anti-CD137 MAb activity are thought to depend on direct killing by $CD8^+$ T cells and NK cells, enhanced proliferation and cytokine secretion by tumor-specific T cells, and Ab-dependent cell-mediated cytotoxicity of NK cells at tumor sites (1). In a mouse B cell lymphoma model, depletion of $CD8^+$ T cells or NK cells abrogated the antitumor effect of anti-CD137 MAb (32). Although the antitumor effect of anti-CD137 MAb is mediated through engagement of $CD8^+$ T cells in most preclinical

tumor models, the role of $CD4^+$ T cells is less clear. Depletion of $CD4^+$ T cells improved the therapeutic efficacy of anti-CD137 MAb in a mouse B cell lymphoma model (32), whereas $CD4^+$ T cells were required for anti-CD137 MAb-induced antitumor immunity in a mouse mastocytoma model (33). Based on our cell depletion experiments, anti-CD137 MAb-mediated clearance of persistent CHIKV RNA was only partially dependent on NK cells and $CD4^+$ and $CD8^+$ T cells. However, anti-CD137 MAb-mediated clearance of CHIKV RNA was abrogated in TCR$\beta\delta^{-/-}$ mice. Immune cell subsets other than conventional $CD4^+$ or $CD8^+$ T cells, such as NKT cells, that are absent in these mice could contribute to anti-CD137 MAb-mediated clearance of CHIKV RNA in the spleen. Because B cells are a major reservoir of persistent CHIKV RNA in the spleen, we hypothesize that anti-CD137 MAb clears persistent CHIKV RNA in the spleen and DLN by targeting B cells. Further study is necessary to define how activation by anti-CD137 MAb induces T cells and possibly NKT cells to lyse and/or to prevent expansion of B cells and to determine whether any of this process is antigen specific.

Our study helps to elucidate the basis for retention of CHIKV RNA in secondary lymphoid tissues. The clearance of CHIKV RNA coincided with a reduction in B cells and FDCs that was mediated by anti-CD137 MAb treatment and T cells. These effects on germinal center formation may be relevant for infections and vaccinations that occur in patients treated with agonistic anti-CD137 MAb therapies for cancers. Although further study is warranted, treatment with anti-CD137 MAbs might blunt the humoral response to newly administered vaccines or infection with pathogens.

MATERIALS AND METHODS

Viruses and cells. A recombinant CHIKV La Reunion (CHIKV-LR) OPY1 strain was provided by S. Higgs (Kansas State University) and generated from *in vitro*-transcribed cDNA as described (34). The resultant virus was propagated once in C6/36 *Aedes albopictus* cells and titrated using Vero cells, as described (35). CHIKV SL15649 was generated in BHK21 cells from *in vitro*-transcribed cDNA, as described (36). The MAYV BeH407 strain was provided by the World Reference Center for Arboviruses (S. Weaver, K. Plante, and R. Tesh) and propagated in Vero cells.

Animal studies. All animal experiments were performed with the approval of Washington University and University of Colorado School of Medicine institutional animal care and use committees, in accordance with their guidelines. C57BL/6J (product no. 000664), B6.129S2-Ighm^{tm1Cgn}/J (μMT) (product no. 002288), and B6.129P2-Tcrb^{tm1Mom} Tcrd^{tm1Mom}/J (TCR$\beta\delta^{-/-}$) (product no. 002121) mice were purchased from the Jackson Laboratory. CD137$^{-/-}$ mice (37) were obtained as a gift from Michael Croft (La Jolla Institute for Immunology). MD4 mice (22) with a μMT B cell-deficient genetic background were generated at the University of Colorado, by crossing mice with the MD4 transgene (product no. 002595; The Jackson Laboratory) with mice of the μMT B cell-deficient background. At 4 weeks of age, male mice anesthetized with ketamine hydrochloride (80 mg/kg body weight) and xylazine (15 mg/kg) were inoculated subcutaneously, in the left rear footpad, with 10^3 focus-forming units (FFU) of CHIKV or MAYV in 10 μl of phosphate-buffered saline (PBS). Foot swelling was measured daily with digital calipers (product no. 54-100-004-2; Fowler). At the termination of experiments, mice were euthanized and perfused with PBS via intracardiac injection. Tissues were harvested and stored at −80°C.

Quantitative reverse transcription-PCR. Viral RNA was extracted from tissue homogenates using the RNeasy minikit (product no. 74182; Qiagen). To extract viral RNA from PFA-fixed cells, the RNeasy kit for purification of total RNA from formalin-fixed, paraffin-embedded tissue sections (product no. 73504; Qiagen) was used, according to the manufacturer's protocol. qRT-PCR was performed using the TaqMan RNA-to-CT 1-step kit (Applied Biosystems) with a CHIKV E1- or MAYV E2-specific primer/probe set (38, 39). The extracted RNA was compared to a standard curve generated with RNA extracted from a CHIKV or MAYV stock, to determine FFU equivalents. To quantify CHIKV genomic and subgenomic RNA levels in the spleen, random primed cDNA was used as a template for CHIKV-sequence-specific forward (CHIKV2444, 5′-TTTGCGTGCCACTCTGG-3′) and reverse (CHIKV2524, 5′-CGGGTCACCACAAAGTACAA-3′) primers and a CHIKV-sequence-specific TaqMan probe (CHIKV2467, 5′-6-carboxyfluorescein [FAM]-ACTT GCTTTGATCGCCTTGGTGAGA-3′) that amplified a region of the nsP2 gene. The same random primed cDNA was also used as a template for CHIKV-sequence-specific forward (CHIKV10239, 5′-CGGCGTCTAC CCATTTATGT-3′) and reverse (CHIKV10363, 5′-CCCTGTATGCTGATGCAAATTC-3′) primers and a CHIKV-sequence-specific TaqMan probe (CHIKV10290, 5′-FAM-AAACACGCAGTTGAGCGAAGCAC-minor groove binder [MGB]-3′) that amplified a region of the E1 gene. A standard curve composed of 10-fold dilutions (from 10^7 to 10^0 copies) of CHIKV positive-strand genomic RNA, synthesized *in vitro* and spiked into RNA from BHK21 cells, was used to determine the nsP1 and E1 gene copy numbers and to confirm that the two assays amplified with similar efficiencies. To determine the relative abundance of the subgenomic RNA, compared with full-length genomic RNA, the data were expressed as a ratio of the E1 gene copy number to the nsP2 gene copy number.

Antibodies and cell depletions. Anti-CD137 MAb (clone 2A, rat Ig2a MAb) has been described previously (40). Antibody was purified from hybridoma supernatants by protein G affinity chromatography, by a commercial vendor (Bio X Cell). Anti-CD4 (clone GK1.5), anti-CD8 (clone YTS169.4), anti-NK1.1

(clone PK136), anti-Ly6G (clone 1A8), anti-CD40L (clone MR-1), rat IgG2b isotype control (clone LTF-2) for $CD4^+$ and $CD8^+$ T cell depletion, mouse IgG2a (clone C1.18.4) for NK and B cell depletion, rat IgG2a isotype control (clone 2A3) for neutrophil depletion, and polyclonal Armenian hamster IgG for CD40L blockade were purchased from Bio X Cell. Anti-CD20 (clone 5D2) was obtained from Genentech. Mice were administered 400 μg of anti-CD137 MAb or rat Ig2a isotype-control MAb (clone 2A3; Bio X Cell), via the intraperitoneal (i.p.) route, at 2 dpi. For cell depletion studies, mice were administered 300 μg of anti-CD4 MAb, 500 μg of anti-CD8 MAb, or 200 μg of anti-NK1.1 MAb at 2 dpi and every 4 days thereafter until 14 dpi or 500 μg of anti-Ly6G antibody at 2 dpi and every 2 days thereafter until 14 dpi. For B cell depletion, mice were administered 200 μg of anti-CD20 MAb at 2 dpi. For CD40L blocking, mice were administered 500 μg of anti-CD40L MAb at 2 dpi and every 3 days thereafter until 14 dpi.

RNA ISH. Uninfected and infected mice were sacrificed and perfused extensively with PBS via intracardiac injection. The spleen was dissected, fixed with 1% PFA in PBS for 2 h at room temperature, and transferred to 10% sucrose in PBS at 4°C. After overnight incubation, tissues were placed overnight in 30% sucrose in PBS at 4°C and then frozen in Tissue-Tek compound (product no. 4583; Sakura) at −80°C. Tissues were cut in 10-μm sections. Viral RNA ISH was performed using RNAscope 2.5 (Advanced Cell Diagnostics), according to the manufacturer's instructions. The probe targeting CHIKV RNA was designed and synthesized by Advanced Cell Diagnostics (product no. 479501). All samples were visualized using a Nikon Eclipse microscope with a QICAM 12-bit camera (QImaging), and results were processed with QCapture software.

Immune cell analysis. Ipsilateral feet from CHIKV-infected mice were skinned and incubated for 2 h at 37°C in 10 ml of digestion buffer (2.5 mg/ml collagenase [Sigma] and 10 μg/ml DNase I [Sigma] in RPMI 1640 medium containing 10% fetal bovine serum [FBS]). The cell suspension was passed through a 70-μm cell strainer. After centrifugation, cells were washed with 1% FBS in Hanks' balanced salt solution, followed by another round of centrifugation and washing. Cells were resuspended in washing buffer (5% FBS in PBS) at 5×10^6 cells/ml and incubated with 2.5 μg of anti-mouse CD16/CD32 antibody (product no. 101302; BioLegend) per 10^6 cells for 20 min on ice. Cells were then stained with Brilliant violet 605 (BV605)-conjugated anti-CD45 (product no. 103140; BioLegend), fluorescein isothiocyanate (FITC)-conjugated anti-CD3ε (product no. 11-0031-85; Invitrogen), phycoerythrin (PE)-conjugated anti-CD4 (product no. 553049; BD Biosciences), peridinin-chlorophyll-protein (PerCP)/Cy5.5-conjugated anti-CD8α (product no. 100734; BioLegend), PE/cyanine 7 (Cy7)-conjugated anti-NK1.1 (product no. 108714; BioLegend), allophycocyanin (APC)/Cy7-conjugated anti-CD19 (product no. 115530; BioLegend), BV421-conjugated anti-Ly6C (product no. 562727; BD Biosciences), or Alexa Fluor 700-conjugated anti-Ly6G (product no. 127622; BioLegend) antibody. Subsequently, cells were fixed and permeabilized with the eBioscience FoxP3/transcription factor staining kit and incubated with Alexa Fluor 647-conjugated anti-FoxP3 antibody (product no. 126408; BioLegend).

Spleens from CHIKV-infected mice were minced and incubated for 30 min at 37°C in 2 ml digestion buffer (1 mg/ml collagenase [Sigma] and 100 μg/ml DNase I [Sigma] in Dulbecco's modified Eagle's medium [DMEM] containing 2% FBS), in a 24-well plate. The cell suspension was passed through a 100-μm cell strainer. After rinsing with 10% FBS, 5 mM EDTA, in DMEM, erythrocytes were lysed for 2 min with 1 ml of ammonium-chloride-potassium (ACK) lysing buffer (Gibco). Cells were washed with DMEM and centrifuged, followed by rinsing with washing buffer (2% FBS, 5 mM EDTA, in PBS). After centrifugation, cells were resuspended in washing buffer at 5×10^8 cells/ml and were incubated for 20 min with 2.5 μg of anti-mouse CD16/CD32 antibody (product no. 101302; BioLegend) per 10^8 cells, on ice. Then, cells were stained with BV605-conjugated anti-CD45 (product no. 103140; BioLegend), PE/Cy7-conjugated anti-CD3 (product no. 100320; BioLegend), APC/Cy7-conjugated anti-CD19 (product no. 115530; BioLegend), PerCP/Cy5.5-conjugated anti-CD11c (product no. 117328; BioLegend), FITC-conjugated anti-CD21/CD35 (product no. 553818; BD Biosciences), BV421-conjugated anti-CD54 (product no. 564704; BD Biosciences), or PE-conjugated anti-CD95 (product no. 554258; BD Biosciences) antibody and biotin-conjugated PNA (product no. B-1075; Vector Laboratories). To confirm CD137 expression, cells were stained with biotin-conjugated anti-CD137 (product no. 106104; BioLegend). Cells were then washed and incubated with Alexa Fluor 647-conjugated streptavidin (product no. S32357; Invitrogen). Subsequently, cells were fixed with BD FACS lysing solution, processed on an LSR Fortessa X-20 (BD Biosciences) flow cytometer, and analyzed using BD FACSDiva and FlowJo software. For fluorescence-activated cell sorting, a BD FACSAria II system was used.

Serum anti-CHIKV IgG ELISA. MaxiSorp 96-well flat-bottomed enzyme-linked immunosorbent assay (ELISA) plates (Thermo Fisher) were coated overnight at 4°C with 2 μg/ml of CHIKV E2 protein (35). Plates were washed with ELISA wash buffer (PBS with 0.05% Tween 20) and blocked with blocking buffer (PBS with 5% FBS) for 4 h at 37°C. Sera from CHIKV-infected mice were added in 3-fold dilutions starting with a 1:100 dilution. After incubation for 1 h at room temperature, plates were washed with ELISA wash buffer. Plates were incubated with biotinylated anti-IgG (product no. 115-065-062; Jackson ImmunoResearch) for 1 h at room temperature. After washing, plates were incubated with streptavidin-conjugated horseradish peroxidase (product no. SA-5004; Vector Laboratories) for 30 min at room temperature. After sequential washes with ELISA buffer and PBS, substrate solution (Thermo Fisher) was added. The reaction was quenched with 2 N H_2SO_4. The plates were read using a Synergy H1 hybrid reader (BioTek). The optical density (OD) (450 nm) value of naive serum was subtracted from the OD values of CHIKV-infected samples, and nonlinear regression curves were calculated. Anti-CHIKV IgG titers were defined as the dilution of serum yielding a half-maximal OD value after background and naive value subtraction.

Statistical analysis. All data were analyzed with GraphPad Prism software. For viral RNA analysis and immune cell analysis, data were analyzed by the Mann-Whitney test, Kruskal-Wallis analysis of variance

(ANOVA) with Dunn's posttest, or two-way ANOVA with Šidák's posttest. *P* values of <0.05 indicate statistically significant differences.

ACKNOWLEDGMENTS

This work was supported by U.S. Public Health Service grants R01 AI141436 (T.E.M. and M.S.D.) and F32 AI122463 (M.K.M.).

M.S.D. is a consultant for Inbios and Emergent BioSolutions and is on the scientific advisory board of Moderna. All other authors declare no potential conflicts of interest.

REFERENCES

1. Yonezawa A, Dutt S, Chester C, Kim J, Kohrt HE. 2015. Boosting cancer immunotherapy with anti-CD137 antibody therapy. Clin Cancer Res 21:3113–3120. https://doi.org/10.1158/1078-0432.CCR-15-0263.
2. Lee SJ, Myers L, Muralimohan G, Dai J, Qiao Y, Li Z, Mittler RS, Vella AT. 2004. 4-1BB and OX40 dual costimulation synergistically stimulate primary specific CD8 T cells for robust effector function. J Immunol 173:3002–3012. https://doi.org/10.4049/jimmunol.173.5.3002.
3. Ito F, Li Q, Shreiner AB, Okuyama R, Jure-Kunkel MN, Teitz-Tennenbaum S, Chang AE. 2004. Anti-CD137 monoclonal antibody administration augments the antitumor efficacy of dendritic cell-based vaccines. Cancer Res 64:8411–8419. https://doi.org/10.1158/0008-5472.CAN-04-0590.
4. Lee H, Park HJ, Sohn HJ, Kim JM, Kim SJ. 2011. Combinatorial therapy for liver metastatic colon cancer: dendritic cell vaccine and low-dose agonistic anti-4-1BB antibody co-stimulatory signal. J Surg Res 169:e43–e50. https://doi.org/10.1016/j.jss.2011.03.067.
5. Cuadros C, Dominguez AL, Lollini PL, Croft M, Mittler RS, Borgstrom P, Lustgarten J. 2005. Vaccination with dendritic cells pulsed with apoptotic tumors in combination with anti-OX40 and anti-4-1BB monoclonal antibodies induces T cell-mediated protective immunity in Her-2/neu transgenic mice. Int J Cancer 116:934–943. https://doi.org/10.1002/ijc.21098.
6. Wei H, Zhao L, Li W, Fan K, Qian W, Hou S, Wang H, Dai M, Hellstrom I, Hellstrom KE, Guo Y. 2013. Combinatorial PD-1 blockade and CD137 activation has therapeutic efficacy in murine cancer models and synergizes with cisplatin. PLoS One 8:e84927. https://doi.org/10.1371/journal.pone.0084927.
7. Staples JE, Breiman RF, Powers AM. 2009. Chikungunya fever: an epidemiological review of a re-emerging infectious disease. Clin Infect Dis 49:942–948. https://doi.org/10.1086/605496.
8. Petersen LR, Powers AM. 2016. Chikungunya: epidemiology. F1000Res 5:82. https://doi.org/10.12688/f1000research.7171.1.
9. Simon F, Javelle E, Oliver M, Leparc-Goffart I, Marimoutou C. 2011. Chikungunya virus infection. Curr Infect Dis Rep 13:218–228. https://doi.org/10.1007/s11908-011-0180-1.
10. Sissoko D, Malvy D, Ezzedine K, Renault P, Moscetti F, Ledrans M, Pierre V. 2009. Post-epidemic chikungunya disease on Reunion Island: course of rheumatic manifestations and associated factors over a 15-month period. PLoS Negl Trop Dis 3:e389. https://doi.org/10.1371/journal.pntd.0000389.
11. Rodriguez-Morales AJ, Cardona-Ospina JA, Villamil-Gómez W, Paniz-Mondolfi AE. 2015. How many patients with post-chikungunya chronic inflammatory rheumatism can we expect in the new endemic areas of Latin America? Rheumatol Int 35:2091–2094. https://doi.org/10.1007/s00296-015-3302-5.
12. Rodriguez-Morales AJ, Villamil-Gomez W, Merlano-Espinosa M, Simone-Kleber L. 2016. Post-chikungunya chronic arthralgia: a first retrospective follow-up study of 39 cases in Colombia. Clin Rheumatol 35:831–832. https://doi.org/10.1007/s10067-015-3041-8.
13. Hoarau J-J, Jaffar Bandjee M-C, Krejbich Trotot P, Das T, Li-Pat-Yuen G, Dassa B, Denizot M, Guichard E, Ribera A, Henni T, Tallet F, Moiton MP, Gauzère BA, Bruniquet S, Jaffar Bandjee Z, Morbidelli P, Martigny G, Jolivet M, Gay F, Grandadam M, Tolou H, Vieillard V, Debré P, Autran B, Gasque P. 2010. Persistent chronic inflammation and infection by chikungunya arthritogenic alphavirus in spite of a robust host immune response. J Immunol 184:5914–5927. https://doi.org/10.4049/jimmunol.0900255.
14. McCarthy MK, Morrison TE. 2017. Persistent RNA virus infections: do PAMPS drive chronic disease? Curr Opin Virol 23:8–15. https://doi.org/10.1016/j.coviro.2017.01.003.
15. Zare F, Bokarewa M, Nenonen N, Bergstrom T, Alexopoulou L, Flavell RA, Tarkowski A. 2004. Arthritogenic properties of double-stranded (viral) RNA. J Immunol 172:5656–5663. https://doi.org/10.4049/jimmunol.172.9.5656.
16. Magnusson M, Zare F, Tarkowski A. 2006. Requirement of type I interferon signaling for arthritis triggered by double-stranded RNA. Arthritis Rheum 54:148–157. https://doi.org/10.1002/art.21517.
17. Hawman DW, Stoermer KA, Montgomery SA, Pal P, Oko L, Diamond MS, Morrison TE. 2013. Chronic joint disease caused by persistent chikungunya virus infection is controlled by the adaptive immune response. J Virol 87:13878–13888. https://doi.org/10.1128/JVI.02666-13.
18. Miner JJ, Cook LE, Hong JP, Smith AM, Richner JM, Shimak RM, Young AR, Monte K, Poddar S, Crowe JE, Jr, Lenschow DJ, Diamond MS. 2017. Therapy with CTLA4-Ig and an antiviral monoclonal antibody controls chikungunya virus arthritis. Sci Transl Med 9:eaah3438. https://doi.org/10.1126/scitranslmed.aah3438.
19. Poo YS, Rudd PA, Gardner J, Wilson JA, Larcher T, Colle MA, Le TT, Nakaya HI, Warrilow D, Allcock R, Bielefeldt-Ohmann H, Schroder WA, Khromykh AA, Lopez JA, Suhrbier A. 2014. Multiple immune factors are involved in controlling acute and chronic chikungunya virus infection. PLoS Negl Trop Dis 8:e3354. https://doi.org/10.1371/journal.pntd.0003354.
20. Carrasco L, Sanz MA, Gonzalez-Almela E. 2018. The regulation of translation in alphavirus-infected cells. Viruses 10:E70. https://doi.org/10.3390/v10020070.
21. Baumjohann D, Preite S, Reboldi A, Ronchi F, Ansel KM, Lanzavecchia A, Sallusto F. 2013. Persistent antigen and germinal center B cells sustain T follicular helper cell responses and phenotype. Immunity 38:596–605. https://doi.org/10.1016/j.immuni.2012.11.020.
22. Mason DY, Jones M, Goodnow CC. 1992. Development and follicular localization of tolerant B lymphocytes in lysozyme/anti-lysozyme IgM/IgD transgenic mice. Int Immunol 4:163–175. https://doi.org/10.1093/intimm/4.2.163.
23. Sun Y, Blink SE, Chen JH, Fu YX. 2005. Regulation of follicular dendritic cell networks by activated T cells: the role of CD137 signaling. J Immunol 175:884–890. https://doi.org/10.4049/jimmunol.175.2.884.
24. Nair S, Poddar S, Shimak RM, Diamond MS. 2017. Interferon regulatory factor-1 protects against chikungunya virus-induced immunopathology by restricting infection in muscle cells. J Virol 91:e01419-17. https://doi.org/10.1128/jvi.01419-17.
25. Young AR, Locke MC, Cook LE, Hiller BE, Zhang R, Hedberg ML, Monte KJ, Veis DJ, Diamond MS, Lenschow DJ. 2019. Dermal and muscle fibroblasts and skeletal myofibers survive chikungunya virus infection and harbor persistent RNA. PLoS Pathog 15:e1007993. https://doi.org/10.1371/journal.ppat.1007993.
26. Suhrbier A, La Linn M. 2004. Clinical and pathologic aspects of arthritis due to Ross River virus and other alphaviruses. Curr Opin Rheumatol 16:374–379. https://doi.org/10.1097/01.bor.0000130537.76808.26.
27. Heinen E, Braun M, Coulie PG, Van Snick J, Moeremans M, Cormann N, Kinet-Denoël C, Simar LJ. 1986. Transfer of immune complexes from lymphocytes to follicular dendritic cells. Eur J Immunol 16:167–172. https://doi.org/10.1002/eji.1830160211.
28. Cinamon G, Zachariah MA, Lam OM, Foss FW, Jr, Cyster JG. 2008. Follicular shuttling of marginal zone B cells facilitates antigen transport. Nat Immunol 9:54–62. https://doi.org/10.1038/ni1542.
29. Batista FD, Harwood NE. 2009. The who, how and where of antigen presentation to B cells. Nat Rev Immunol 9:15–27. https://doi.org/10.1038/nri2454.
30. Hanna MG, Jr, Szakal AK. 1968. Localization of ^{125}I-labeled antigen in germinal centers of mouse spleen: histologic and ultrastructural autoradiographic studies of the secondary immune reaction. J Immunol 101:949–962.

31. Heesters BA, Lindqvist M, Vagefi PA, Scully EP, Schildberg FA, Altfeld M, Walker BD, Kaufmann DE, Carroll MC. 2015. Follicular dendritic cells retain infectious HIV in cycling endosomes. PLoS Pathog 11:e1005285. https://doi.org/10.1371/journal.ppat.1005285.
32. Houot R, Goldstein MJ, Kohrt HE, Myklebust JH, Alizadeh AA, Lin JT, Irish JM, Torchia JA, Kolstad A, Chen L, Levy R. 2009. Therapeutic effect of CD137 immunomodulation in lymphoma and its enhancement by Treg depletion. Blood 114:3431–3438. https://doi.org/10.1182/blood-2009-05-223958.
33. Melero I, Shuford WW, Newby SA, Aruffo A, Ledbetter JA, Hellstrom KE, Mittler RS, Chen L. 1997. Monoclonal antibodies against the 4-1BB T-cell activation molecule eradicate established tumors. Nat Med 3:682–685. https://doi.org/10.1038/nm0697-682.
34. Tsetsarkin K, Higgs S, McGee CE, De Lamballerie X, Charrel RN, Vanlandingham DL. 2006. Infectious clones of chikungunya virus (La Reunion isolate) for vector competence studies. Vector Borne Zoonotic Dis 6:325–337. https://doi.org/10.1089/vbz.2006.6.325.
35. Pal P, Dowd KA, Brien JD, Edeling MA, Gorlatov S, Johnson S, Lee I, Akahata W, Nabel GJ, Richter MK, Smit JM, Fremont DH, Pierson TC, Heise MT, Diamond MS. 2013. Development of a highly protective combination monoclonal antibody therapy against chikungunya virus. PLoS Pathog 9:e1003312. https://doi.org/10.1371/journal.ppat.1003312.
36. Morrison TE, Oko L, Montgomery SA, Whitmore AC, Lotstein AR, Gunn BM, Elmore SA, Heise MT. 2011. A mouse model of chikungunya virus-induced musculoskeletal inflammatory disease: evidence of arthritis, tenosynovitis, myositis, and persistence. Am J Pathol 178:32–40. https://doi.org/10.1016/j.ajpath.2010.11.018.
37. Kwon BS, Hurtado JC, Lee ZH, Kwack KB, Seo SK, Choi BK, Koller BH, Wolisi G, Broxmeyer HE, Vinay DS. 2002. Immune responses in 4-1BB (CD137)-deficient mice. J Immunol 168:5483–5490. https://doi.org/10.4049/jimmunol.168.11.5483.
38. Bellini R, Medici A, Calzolari M, Bonilauri P, Cavrini F, Sambri V, Angelini P, Dottori M. 2012. Impact of chikungunya virus on *Aedes albopictus* females and possibility of vertical transmission using the actors of the 2007 outbreak in Italy. PLoS One 7:e28360. https://doi.org/10.1371/journal.pone.0028360.
39. Long KC, Ziegler SA, Thangamani S, Hausser NL, Kochel TJ, Higgs S, Tesh RB. 2011. Experimental transmission of Mayaro virus by *Aedes aegypti*. Am J Trop Med Hyg 85:750–757. https://doi.org/10.4269/ajtmh.2011.11-0359.
40. Wilcox RA, Flies DB, Zhu G, Johnson AJ, Tamada K, Chapoval AI, Strome SE, Pease LR, Chen L. 2002. Provision of antigen and CD137 signaling breaks immunological ignorance, promoting regression of poorly immunogenic tumors. J Clin Invest 109:651–659. https://doi.org/10.1172/JCI14184.